Existence of Superstructures Due to Large Amounts of Fe Vacancies in the LiFePO4-Type Framework

ARTICLE *in* CHEMISTRY OF MATERIALS · DECEMBER 2010

Impact Factor: 8.35 · DOI: 10.1021/cm102511m

6 AUTHORS, INCLUDING:

Montse Casas-Cabanas
CIC Energigune
39 PUBLICATIONS **1,114** CITATIONS
SEE PROFILE

Loic Dupont
Université de Picardie Jules Verne
128 PUBLICATIONS **7,157** CITATIONS
SEE PROFILE

Carine Davoisne
Université de Picardie Jules Verne
36 PUBLICATIONS **450** CITATIONS
SEE PROFILE

Christian Masquelier
Université de Picardie Jules Verne
165 PUBLICATIONS **7,514** CITATIONS
SEE PROFILE

32 *Chem. Mater.* **2011,** *23,* 32–38
DOI:10.1021/cm102511m

CHEMISTRY OF MATERIALS
Article

Existence of Superstructures Due to Large Amounts of Fe Vacancies in the $LiFePO_4$-Type Framework

S. Hamelet,[†] M. Casas-Cabanas,[‡,§] L. Dupont,[†] C. Davoisne,[†] J. M. Tarascon,[†] and C. Masquelier*,[†]

[†]*Laboratoire de Réactivité et Chimie des Solides, Université de Picardie Jules Verne, 33 Rue Saint-Leu, 80039, Amiens Cedex, France, and* [‡]*Electron Microscopy for Materials Science (EMAT), University of Antwerp, Belgium.* [§]*Present address: Laboratoire Cristallographie et sciences des Matériaux, 6 Boulevard du Maréchal Juin - F-14050 CAEN cedex 4 France.*

Received September 1, 2010. Revised Manuscript Received November 3, 2010

$LiFePO_4$ has been under intense scrutiny over the past decade because it stands as an attractive positive electrode material for the next generation of Li-ion batteries to power electric vehicles and hybrid electric vehicles, hence the importance of its thermal behavior. The reactivity of $LiFePO_4$ with air at moderate temperatures is shown to be dependent on its particle size. For nanosized materials, a progressive displacement of Fe from the core structure leading to a composite made of nanosize Fe_2O_3 and highly defective, oxidized $Li_xFe_yPO_4$ compositions, among which the "ideal" formula $LiFe_{2/3}PO_4$. Herein we report, from both temperature-controlled X-ray diffraction and electronic diffraction microscopy, that these off-stoichiometry olivine-type compounds show a defect ordering resulting in the formation of a superstructure. Such a finding shows striking similarities with the temperature-driven oxidation of fayalite Fe_2SiO_4 (another olivine) to structurally defective laihunite, reported in the literature three decades ago.

Introduction

In the Li-ion energy storage field, $LiMPO_4$ (with M = Fe, Mn, Co, Ni) olivine-type materials have been the center of enormous scientific attention for more than ten years after the pioneering works of Padhi et al.[1,2] and Ravet et al.[3] After a great worldwide attention,[4−13] these materials are now becoming the most attractive positive electrodes for power tools and hybrid vehicle applications[14,15] and are a commercial reality. The benefits of using $LiFePO_4$ in Li-ion batteries are its excellent cycle life, the structural stability of the delithiated $FePO_4$ phase upon heating and the low cost of its raw materials components. Recent developments show the possibility of drastically increasing power densities.[16] Some groups succeeded to overcome (i) its low operating voltage (3.45 V vs Li^+/Li^0) by substituting a part of the iron with another transition metal[17] and (ii) its low total electrical conductivity ($\sim 10^{-9}$ S.cm^{-1} at 298 K) by either carbon coating,[10,11] doping with several elements,[5,18] or by particles downsizing.[4,7,8,12−14]

Regarding the latter, high-surface $LiMPO_4$ powders made of nanoparticles containing significant amounts of structural defects within the triphylite structure were prepared by several groups via novel low-temperature synthesis routes. Our group suggested[19] that the presence of Fe and vacancies in the Li crystallographic sites had a dramatic effect on the electrochemical behavior: a full reversible solid solution mechanism was found at 298 K upon electrochemical lithium insertion/deinsertion.

However, another important question still remains concerning the benefits or drawbacks of using nanoparticles with enhanced reactivity of surfaces. Martin et al.

*To whom correspondence should be addressed. E-mail: christian.masquelier@u-picardie.fr.

(1) Padhi, A. K.; Nanjundaswamy, K. S.; Goodenough, J. B. *J. Electrochem. Soc.* **1997**, *144*, 1188.
(2) Goodenough, J. B.; Padhi, A.; Nanjundaswamy, K. S.; Masquelier, C. World Patent WO9740541, 1997.
(3) Ravet, N.; Goodenough, J. B.; Besner, S.; Simoneau, M.; Hovington, P.; Armand, M. Abstract No. 127, 196th Meeting of the Electrochemical Society, HI, 1999.
(4) Yamada, A.; Chung, S. C.; Hinokuna, K. *J. Electrochem. Soc.* **2001**, *148*, A224.
(5) Herle, S. P.; Ellis, B.; Coombs, N.; Nazar, L. F *Nat. Mater.* **2004**, *3*, 147.
(6) Yang, S.; Zavalij, P. Y.; Whittingham, M. S. *Electrochem. Commun.* **2001**, *3*, 505–508.
(7) Delacourt, C.; Poizot, P.; Levasseur, S.; Masquelier, C. *Electrochem. Solid State Lett.* **2006**, *9*(7), A352–A355.
(8) Nuspl, G.; Wimmer, L.; Eisgruber, M. World Patent WO 2005/051840 A1, 2005.
(9) Kim, D. H.; Kim, J. *Electrochem. Solid State Lett.* **2006**, *9*(9), A439–A442.
(10) Armand, M.; Gauthier, M.; Magnan, J. F.; Ravet, N. World Patent WO 02/27823 A1, 2002.
(11) Dominko, R.; Gaberscek, M.; Drofenik, J.; Bele, M.; Pejovnik, S. *Electrochem. Solid State Lett.* **2001**, *4*, A187–A190.
(12) Delacourt, C.; Poizot, P.; Masquelier, C. World Patent WO 2007/000251A1, 2007.
(13) Gaberscek, M.; Dominko, R.; Jamnic, J. *Electrochem. Commun.* **2007**, *9*, 2778–2783.
(14) Meetong, N.; Huang, H.; Speakman, S.; Carter, W. C.; Chiang, Y. M. *Adv. Funct. Mater.* **2007**, *17*, 1115–1123.
(15) Chiang, Y-M; Gozdz, A. S.; Payne, M. W. U.S. Patent US2007/0031732A1, 2007.
(16) Kang, B.; Ceder, G. *Nature* **2009**, *458*, 190.
(17) Yamada, A.; Takei, Y; Koizumi, H.; Sonoyama, N.; Kanno, R. *Appl. Phys. Lett.* **2005**, *87*, 252503.
(18) Chung, S. Y.; Bloking, J. T.; Chiang, Y. M. *Nat. Mater.* **2002**, *1*, 123.
(19) Gibot, P.; Casas-Cabanas, M.; Laffont, L.; Levasseur, S.; Carlach, P.; Hamelet, S.; Tarascon, J.-M.; Masquelier, C. *Nat. Mater.* **2008**, *7*, 741–747.

 Published on Web 12/14/2010

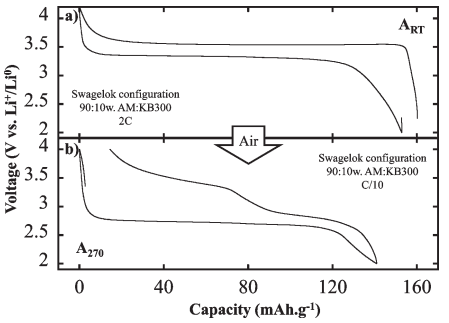

Figure 1. Effect of thermal treatment under air on LFP-type electrodes. Carbon-coated LFP (A_{RT}) is transformed to a highly defective LFP (A_{270}) with completely new electrochemical behavior.[22]

described a deintercalation process occurring with $LiFePO_4$/C nanocomposites because of air exposure.[20] The formation of a partially hydrated $Li_xFePO_4(OH)_x$ phase leading to an electrochemical performance loss was also proposed.[21] Our recent finding had also confirmed that olivine compounds were very sensitive to moderate thermal treatments in air,[22] and a different mechanism was put forward. It involves the oxidation of $LiFePO_4$, which leads to iron extrusion toward the particle surface and hence to Fe vacancies. It was then possible to obtain a pure Fe^{III} olivine, where 1/3 of the iron initially contained in the $LiFePO_4$ pristine particles had been extruded to form nanoclusters of Fe_2O_3. In this case again, this important amount of structural defects led to a completely unexpected electrochemical behavior, with two solid-solution redox reactions, around 3.4 and 2.7 V vs Li^+/Li^0 (Figure.1) and anisotropic variations of the lattice parameters during charge and discharge.[22]

In this paper, we report on the experimental discovery, through X-ray diffraction and transmission electron microscopy, of new structural forms of $LiFePO_4$ built on Olivine-type frameworks, similar to what had been reported previously for Fayalite Fe_2SiO_4 by Kondoh et al.[23] We show for the first time that Fe extrusion generates indeed complex superstructures of the triphylite-type framework for $LiFe_{1-y}PO_4$ due to Fe/vacancy ordering and possible Li ⇔ Fe exchange.

Experimental Section

A pristine "$LiFePO_4$" powder (LFP_{RT}) was obtained by direct precipitation under ambient atmosphere, slightly above 100 °C.[7,12] Aqueous solution mixtures containing 0.1 mol·L^{-1} of Fe^{II} sulfate ($FeSO_4 \cdot 7H_2O$, Sigma Aldrich) and 0.1 mol·L^{-1} of H_3PO_4 (Baker) were brought to an optimal pH value, close to neutrality, by slowly adding 0.3 mol L^{-1} of lithium hydroxide ($LiOH \cdot H_2O$, Alfa Aesar). This resulted in the formation of greenish particles, which were subsequently kept under refluxing conditions for about 12 h. under mechanical stirring before being recovered by centrifugation and dried.

Following our previous report on selective oxidation of LFP-type powders under air, we carefully annealed significant quantities of LFP_{RT} under air (12 h) at various temperatures (XXX°C) so as to produce different series of "oxidized" $Li_{1-\varepsilon}Fe_{1-y}PO_4$ powders ($0.33 > y > \varepsilon > 0$), labeled as LFP_{XXX}.

Pristine Fe_2SiO_4 was synthesized via a solid−solid reaction under Ar at 750 °C, between a stoichiometric mixture of SiO_2, nano-Fe_2O_3, and Fe as previously described.[24] SiO_2 nanopowders were prepared via hydrolysis of tetraethoxysilane (TEOS) in water−ethanol (1−5) mixture in presence of a few drops of ammoniac (NH_4OH) as catalyst to promote room temperature precipitation. Once recovered, the precipitate was heated to 400 °C for 2 h. Nano-Fe_2O_3 had been synthesized by "flash" heating of $Fe_2C_2O_4.2H_2O$ at 400 °C under air. Fe was purchased by Sigma Aldrich.

Two samples were selected, LFP_{270} and LFP_{400}, for in-depth X-ray diffraction and transmission electron microscopy studies.

X-ray powder diffraction (XRD) diagrams were collected on a Bruker D8 diffractometer (40 kV, 40 mA), using the Co Kα radiation, a Göbel mirror, and a Braun PSD detector, mounted in a $\theta-\theta$ configuration. The thermal behavior was followed in situ by performing temperature-controlled X-ray diffraction in the above-mentioned X-ray diffractometer using an HTK 1200 °C Anton Parr Chamber. Each pattern was recorded for approximately 45 min at constant temperature, between $2\theta = 5°$ and $2\theta = 32°$ with steps of 0.032°/s. Between each programmed temperatures, the heating rate was 0.5 °C/min. The same conditions were used for cooling.

The morphology, size, and elemental compositions of the samples were characterized by scanning electron microscopy (SEM) using a FEI Quanta 200F microscope equipped with a Link Isis apparatus (Oxford) for energy dispersive X-ray spectroscopy (EDX). High-resolution transmission electron microscopy (HRTEM) imaging and electron energy loss spectroscopy (EELS) analyses were performed using a FEI Tecnai F20 S-TWIN operating at 200 kV fitted with an EDX detector and a Gatan Image Filter Tridiem in post column. Electron diffraction patterns were obtained through selected area electron diffraction (SAED). For these experiments, samples had been previously dispersed in methanol and deposited on copper grids with holey carbon. For the EELS spectra acquisition, the following conditions were used: a dispersion of 0.1 eV/channel and a resolution of 0.9 eV determined by measuring the full width at half-maximum of the zero-loss peak. The energy loss near edge structure (ELNES) acquisitions were done in STEM mode using point analysis. Background subtraction considering a power law function and energy correction with respect to the O−K edge main feature at 539 eV for the LFP_{RT} sample and prepeak at 532 eV for the LFP_{400} have been performed.

Results and Discussion

As described extensively in our previous publication[22] the annealing in air of $LiFePO_4$ powders up to 270 °C results in significant unit-cell volume contraction that starts as soon as ∼140 °C for nanosized powders. This unit-cell contraction is associated with progressive oxidation of the powder caused by Fe extrusion to form Fe_2O_3

(20) Martin, J. F.; Yamada, A.; Kobayashi, G.; Nishimura, S.-I.; Kanno, R.; Guyomard, D.; Dupré, N. *Electrochem. Solid-State Lett*. **2008**, *11*(1), A12–A16.
(21) Cuisinier, M.; Martin, J.-F.; Dupré, N.; Yamada, A.; Kanno, R.; Guyomard, D. *Electrochem. Commun*. **2010**, *12*(2), 238–241.
(22) Hamelet, S.; Gibot, P.; Casas-Cabanas, M.; Bonnin, D.; Grey, C. P.; Cabana, J.; Leriche, J.-B.; Rodriguez-Carvajal, J.; Courty, M.; Levasseur, S.; Carlach, P.; Van-Thournout, M; Tarascon, J.-M.; Masquelier, C. *J. Mater. Chem*. **2009**, *19*, 3979–3991.
(23) Kondoh, S.; Kitamura, M.; Mojimoto, N. *Am. Mineral*. **1985**, *70*, 737–746.
(24) Recham, N.; Casas-Cabanas, M.; Cabana, J.; Grey, C. P.; Jumas, J. C.; Dupont, L.; Armand, M.; Tarascon, J. M. *Chem. Mater*. **2008**, *20*, 6798–6809.

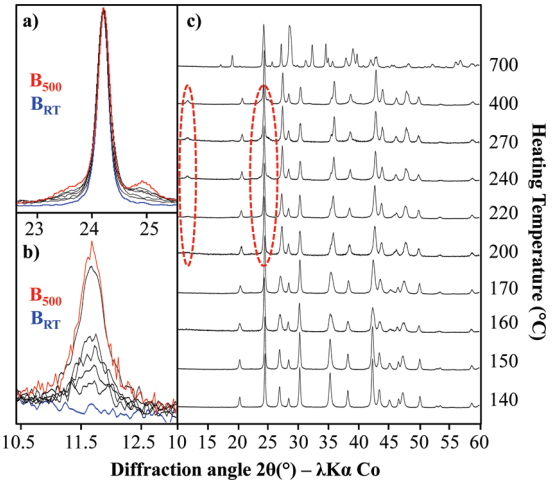

Figure 2. Pristine sample LFP_{RT} heated under air at different temperatures and measured subsequently at room temperature. (a and b):Close up of the extra peaks growing as a function of *T*.

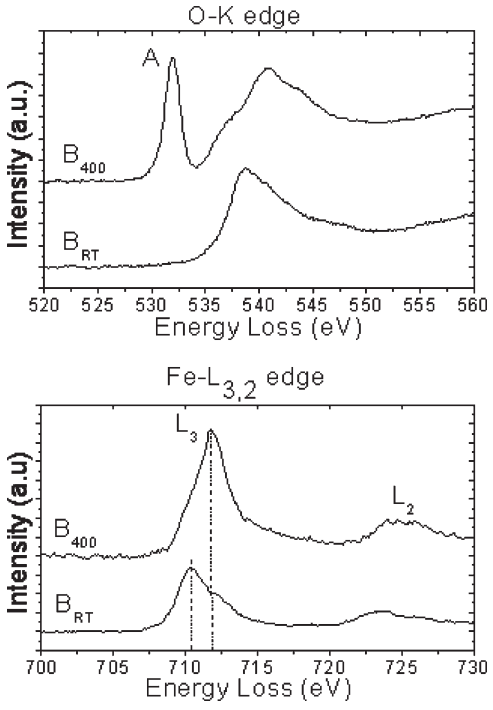

Figure 3. O−K and Fe−$L_{3,2}$ edge spectra of the pristine $LiFePO_4$ (LFP_{RT}) and of the $LiFePO_4$ annealed at 400 °C (LFP_{400}).

and a defective $LiFe_{1-y}PO_4$ triphylite-based composition. From ~550 °C, the overall reaction $3LiFePO_4 \rightarrow Li_3Fe_2(PO_4)_3 + 1/2Fe_2O_3$ has been completed (Figure 2).

An EELS study has been undertaken to determine the evolution of the iron environment in pristine $LiFePO_4$ and sample LFP_{400}. Figure 3 shows O−K and Fe−$L_{3,2}$ edge spectra in the pristine and oxidized $LiFePO_4$. The peaks labeled L_3 and L_2 in the Fe $L_{3,2}$ edge spectra correspond to the spin orbit splitting of the 2p core hole.

The shape of the oxygen edge for the pristine sample is representative of the one in $LiFePO_4$.[25] In iron oxide compounds, the intensity of the peak labeled A in the O−K edge increases with the Fe^{3+} content.[26,27] The high intensity of this feature in the LFP_{400} sample is in accord with the presence of Fe^{3+}. A shift of 1,5 eV is observed for the Fe L_3 line between LFP_{RT} and LFP_{400}, which corresponds to a chemical shift due to a change in the iron oxidation state from +II to +III.[28,29] The LFP_{RT} Fe L_3 line in the Fe edge spectra is composed of a sharp maximum followed by a shoulder that is characteristic of Fe^{2+}.[25] The LFP_{400} Fe L_3 line is composed of a weak feature leading the main feature that corresponds to the Fe^{3+} shape. These observations are in agreement with the oxidation of the iron in the structure during thermal annealing.

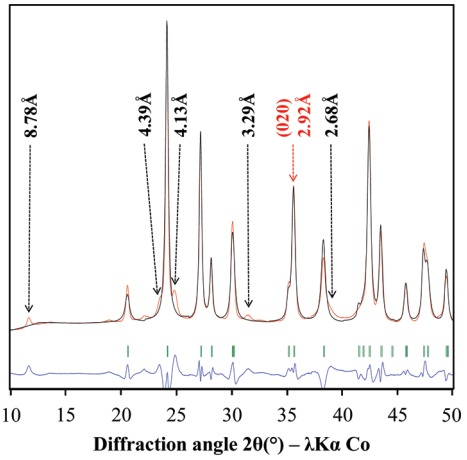

Figure 4. Full-pattern matching refinement of LFP_{400} sample using a "standard" triphylite unit-cell in *Pnma* space group. Red line: Experimental data. Black line: Refinement. Blue line: Difference between experimental and refinement intensities. Green: Bragg's positions.

Our new finding, highlighted in Figure 2, is that new diffraction lines progressively grow in specific d_{hkl} regions from around 200−400 °C and disappear when the defective triphylite-type phase decomposes to $Li_3Fe_2(PO_4)_3$. Their intensities are rather small, and the most obvious observation is that one of them pops up at rather low diffraction angle, that is, big d_{hkl} value. These reflections do not correspond to diffraction peaks of Fe_2O_3, which made us envisage immediately the existence of a superstructure.

The X-ray diffraction full-pattern matching refinement of the LFP sample annealed in air at 400 °C, LFP_{400}, using a "classical" *Pnma* unit-cell (a = 10.017(2) Å, b = 5.853(4) Å, c = 4.728(1) Å) is shown in Figure 4. The superstructure peaks are clearly visible. Indeed, the diffraction peak at $2\theta_{CoK\alpha} = 11.66°$ corresponds to a d_{hkl} value of 8.78 Å that is exactly 3 × 2.92, that is, 3 × d_{020} or a d_{hkl} value of 4.39 Å, exactly half of 8.78 Å.

We then performed a full-pattern refinement of LFP_{400} sample in the space group *Pnma* with a triple-cell superstructure along the *b* direction. As seen in Figure 5a, most of the "new" additional diffraction peaks are nicely

(25) Laffont, L.; Delacourt, C.; Gibot, P.; Wu, M. Y.; Kooyman, P.; Masquelier, C.; Tarascon., J. M. *Chem. Mater.* **2006**, *18*, 5520–5529.
(26) Calvert, C. C.; Brown, A.; Brydson, R. *J. Electron Spectrosc. Relat. Phenom.* **2005**, *143*, 173–187.
(27) Colliex, C.; Manoubi, T.; Ortiz, C. *Phys. Rev. B* **1991**, *44*, 11402–11411.
(28) van Aken, P. A.; Liebscher, B. *Phys. Chem. Miner.* **2002**, *29*, 188–200.
(29) Garvie, L. A. J.; Craven, A. J.; Brydson, R. *Am. Mineral.* **1994**, *79*, 411–425.

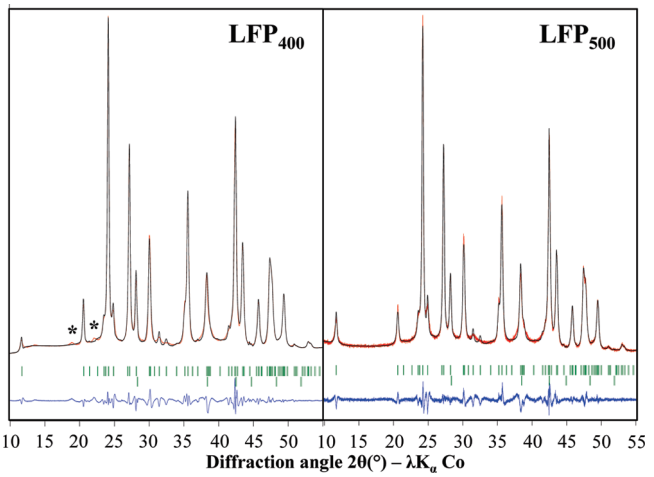

Figure 5. Full-pattern matching refinement of (a) LFP_{400} and (b) LFP_{500} samples using a 3-fold (along *b*) triphylite unit-cell in *Pnma* space group. Red line: Experimental data. Black line: Refinement. Blue line: Difference between experimental and refinement intensities. Green: Bragg's positions.

indexed in such cell, with refined final lattice parameters: $a = 10.015(2)$ Å, $b = 17.558(3)$ Å, and $c = 4.727(1)$ Å. One has to realize, however, that the fit is not yet perfect as two small-intensity broad peaks, identified with stars, are not indexed. Figure 5b shows the same kind of refinement for sample LFP_{500}, that is, annealed at 500 °C, for which these broad weak reflections are not present anymore. From the comparison of these two samples, we may argue that an intermediate or not well-defined superstructure is obtained at 400 °C and that the ordering is more straightforward at 500 °C that would correspond to a composition close to $LiFe_{2/3}PO_4$.

To confirm these findings, we undertook a detailed electronic diffraction study of LFP_{XXX} samples annealed at various temperatures, i.e. with possible different compositions. As seen by the SEM image of Figure 6a, the pristine particles of $LiFePO_4$ are in the range of 150−250 nm in size and it is striking to observe particles with very irregular shapes and "holes" after annealing at 270 (Figure 6b) or 400 °C (Figure 6c) under air. We observed this feature for many particles of many powders investigated without, at this point, reaching a precise understanding of the underpinning science accounting for these morphology changes. In light of what had been published[30−32] previously on morphology features of $LiFePO_4$ particles, it would be certainly interesting in the future to try to model which surfaces would be more prone to oxidation. Once we made sure that these unusual particle shapes do not result from the interaction with the electron beam, we may suggest then that they are associated with the oxidation mechanism itself, that is, the creation of significant amounts of Fe vacancies and Li ⇔ Fe exchange coupled with Fe "extrusion", as evidenced previously through Mössbauer spectroscopy.[22] Note that additional

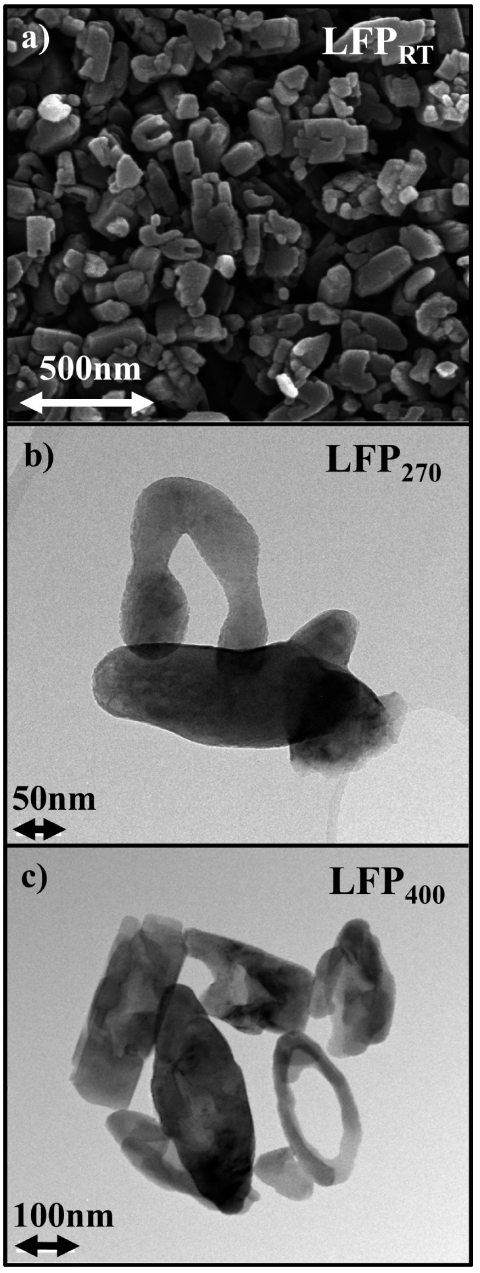

Figure 6. SEM and TEM images of LFP particles. (a) Pristine $LiFePO_4$ prior to annealing, (b) annealed at 270 °C, and (c) annealed at 400 °C.

experimental proof of Li/Fe "antisite" exchange has been reported by Chung et al.[33] and modeled by Fisher et al.[34]

Figure 7 shows two electron diffraction patterns of pristine $LiFePO_4$ and after annealing at 400 °C under air, recorded during the electron crystallographic study made by tilting along the [010]* direction in order to reconstruct the reciprocal space. These two patterns were recorded along the [10−1] zone axis. They complement very satisfactorily the indexation of the X-ray diffraction patterns presented in Figures 4 and 5. The hkl indices, reported in white colors refer to the indexation of the pattern within the LFP "standard" unit-cell ($a = 10.02$, $b = 5.85$, $c = 4.73$). Note that the observed

(30) Ellis, B.; Subramanya Herle, P.; Rho, Y. H.; Nazar, L. F.; Dunlap, R.; Perry, L. K.; Ryan, D. H. *Faraday Discuss.* **2007**, *134*, 119–141.
(31) Chen, G.; Song, X.; Richardson, T. J. *J. Electrochem. Soc.* **2007**, *154*, A627.
(32) Fisher, C. A. J.; Islam, M. S. *J. Mater. Chem.* **2008**, *18*, 1209–1215.
(33) Chung, S. Y.; Choi, S. Y.; Yamamoto, T.; Ikuhara, Y. *Phys. Rev. Lett.* **2008**, *100*, 125502.
(34) Fisher, C. A. J.; Hart Prieto, V. M.; Islam, M. S. *Chem. Mater.* **2008**, *20*, 5907–5915.

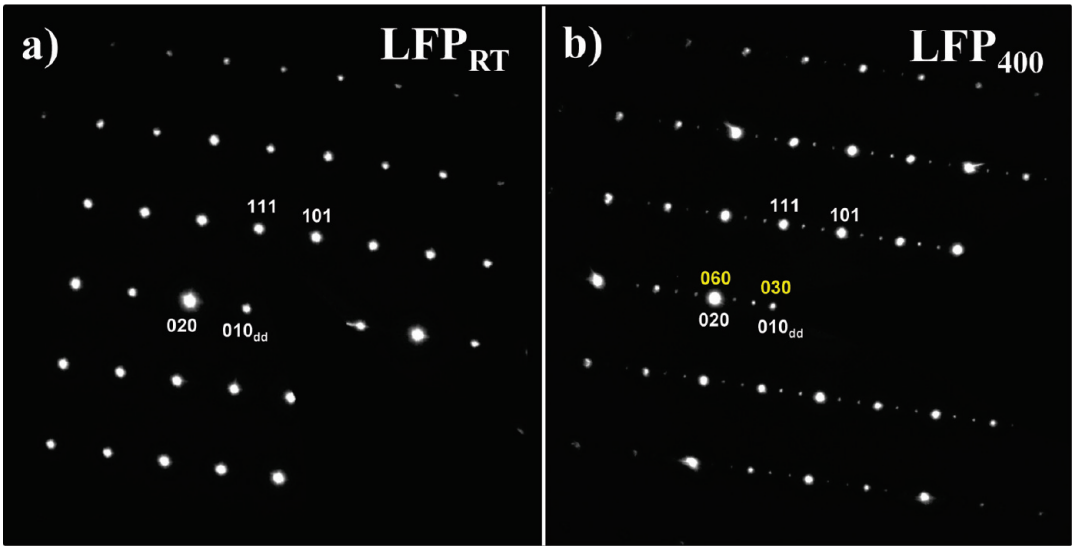

Figure 7. [10−1]* zone axis electron diffraction patterns recorded on (a) pristine $LiFePO_4$ and (b) Sample LFP_{400}.

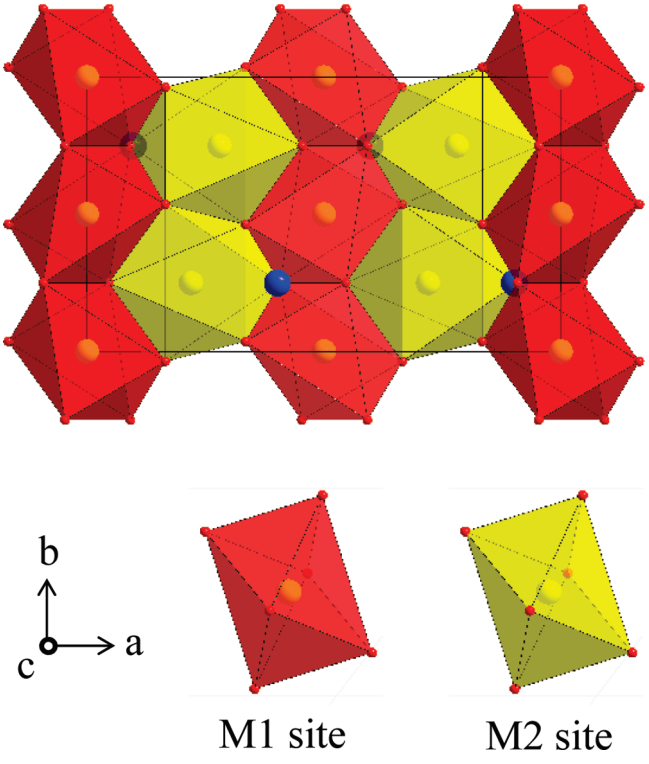

Figure 8. Crystal structure of Fayalite Fe_2SiO_4. Red: M(1) sites occupied by Fe. Yellow: M(2) sites occupied by Fe.

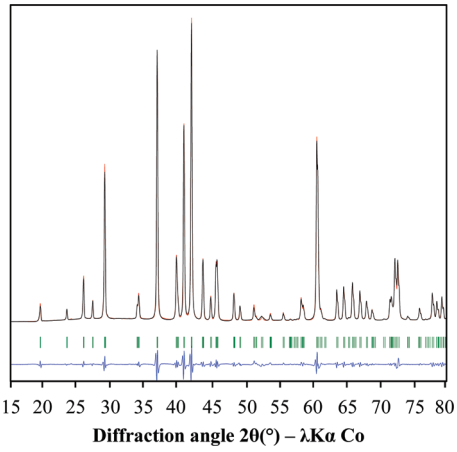

Figure 9. Full-pattern matching refinement of pure Fayalite Fe_2SiO_4 in the space group *Pnma*.

forbidden $(0k0)^*$ $k = 2n + 1$ reflections are observed, on both patterns, because of the double diffraction phenomena. By comparing both patterns an extra set of spots is observed along the [010]* direction (Figure 7b) resulting to the first observation of a triple-cell superstructure along the *b* direction (*Pnma* description) of a triphylite-based powder. To index all the reflections, the *k* index should be multiplied by 3 (yellow setting).

As first mentioned in our previous paper,[22] the oxidation of $LiFePO_4$ in air is associated with low-temperature chemical diffusion of Fe^{II} species, which had been previously reported to occur in another olivine-type structure: Kondoh et al.,[23] among others, indeed demonstrated that fayalite Fe_2SiO_4 transforms into laihunite $Fe_{2-x}SiO_4$ upon oxidation, concomitant with the formation of SiO_2 and iron oxide. The mineral Laihunite had been found in 1976 in China by the Laihunite Research Group[35] as a minor constituent of a quartz hypersthene granulite and often associated with fine-grained magnetite inclusions.[36] This discovery is a very interesting illustration of the extensively rich crystal chemistry of olivine-type structures dealing with occupancies and ordering of divalent cations on octahedral sites.

The oxidation of fayalite Fe_2SiO_4, whose structure is represented in figure 8, occurs progressively as a function of temperature to yield $\square_x Fe^{2+}_{2-3x}Fe^{3+}_{2x}SiO_4$ up to the "ideal" laihunite formula $Fe^{2+}_{0.5}Fe^{3+}_{1.0}SiO_4$ into which all M2 octahedral positions are occupied by Fe^{3+}, whereas M1 octahedral positions are alternately vacant

(35) Laihunite Research Group. Geochimica **1976**, *2*, 95−103.
(36) Kitamura, M.; Shen, B.; Banno, S.; Morimoto, N. *Am. Mineral.* **1984**, *69*, 154–160.

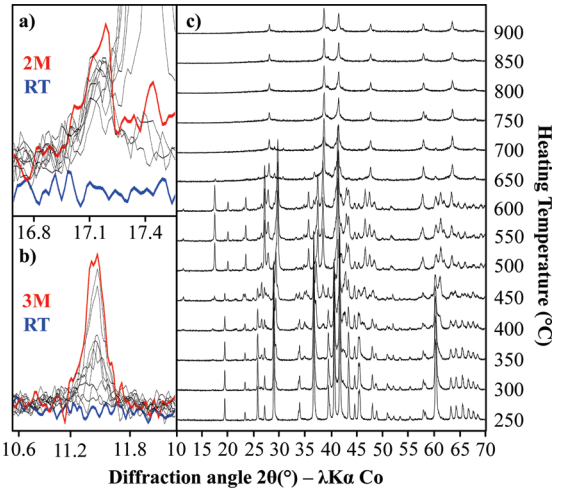

Figure 10. Temperature-controlled X-ray diffraction under air of Fe_2SiO_4.

and occupied by Fe^{2+}. Tamada et al.[37] determined the average structure of laihunite in the monoclinic space group $P2_1/b$ (a = 4.805(2) Å, b = 10.189(9) Å, c = 5.801(1) Å, α = 91.0(2)°), isostructural with sarcopside $(Fe,Mn)_3(PO_4)_2$.

To establish a close parallel with what we observed upon heating $LiFePO_4$ in air, we performed a temperature-controlled X-ray diffraction experiment in air for Fayalite Fe_2SiO_4. As seen in Figure 9, the pristine Fe_2SiO_4 used was of high purity as a result of a careful synthesis procedure and its XRD pattern was fully indexed in the orthorhombic space group *Pnma* with a = 10.479(1) Å, b = 6.0918(4) Å, and c = 4.8203(9) Å.

The X-ray diffraction patterns collected upon heating Fe_2SiO_4 in air between 50 and 900 °C are gathered in Figure 10. Compared with the pristine powder, additional diffraction peaks start to appear from 300 to 350 °C Similar with what we observed for $LiFePO_4$, the appearance of the satellite peaks is associated with a significant contraction of the fayalite-type unit-cell because of the oxidation of Fe when it is "extruded" from the structure.

Besides the diffraction peak attributed to Fe_2O_3 at 2θ = 8.57° (d = 11.97 Å), we clearly identified the formation of additional diffraction peaks at 2θ = 17.45° (d = 5.89 Å) and 2θ = 11.44° (d = 8.97 Å) characteristic of the so-called Laihunite-2 M and Laihunite-3 M superstructures. Shen et al.[38] and Li et al.[39] indeed reported first the existence of satellite reflections along c^* (in $P2_1/b$ notation) indicating superlattice structures within a distorted olivine type structure, with a 2-fold supercell (Laihunite-2M) or 3-fold supercell (Laihunite-3M), as reviewed by Kondoh.[23] The superstructure of Laihunite-3 M has been determined by Shen et al.[40] from a twinned single-crystal X-ray diffraction study,

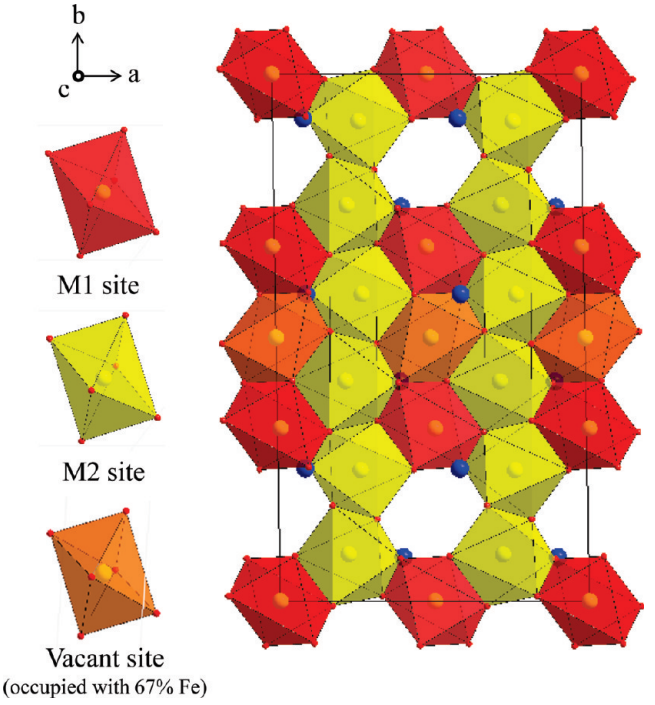

Figure 11. Crystal structure of Laihunite-3 M as determined by Shen et al.[35] used as a model for the newly found superstructure of $LiFe_{2/3}\square_{1/3}PO_4$.

in the space group $P2_1/b$ with a = 4.805(2) Å, b = 10.189(9) Å, c = 17.403(9) Å, α = 91.0(2)°. As seen in Figure 11, a 3-fold supercell along c is necessary to describe this structure with a peculiar distribution of Fe and vacancies onto the M(1) and M(2) sites of the olivine framework. Several models of distribution of cations and vacancies into the laihunite structure are presented by Janney et al.[41]

Conclusion

This study reveals, for the first time to our knowledge, the existence of a new structural form derived from triphylite $LiFePO_4$, obtained by controlled oxidation in air. The oxidation of $LiFePO_4$ in air results in Fe extrusion and concomitant oxidation of the remaining Fe in the structure. The present study reveals, as we pointed out from precise analysis of Mössbauer data,[22] that Fe atoms are redistributed onto the M(1) and M(2) sites and lead, when significant amounts of Fe vacancies have been created, to complex superstructures similar to what had been previously described for the transformation of fayalite to laihunite.[36,41] As developed by Kondoh,[23] the oxidation of fayalite may result in complex intergrowths of 2M- and 3M-layunites, and we indeed observed both forms present simultaneously around 450 °C. One should note that the occurrence of these superstructures appears in our case at significantly lower temperatures than reported by Kondoh, probably consistent with much smaller pristine Fe_2SiO_4 particles in our case (~700 nm vs 2 μm).

At this point, because of the complexity of the new $Li_{1-\varepsilon}Fe_{1-y}PO_4$ ($0.33 > y \gg \varepsilon > 0$) structures observed

(37) Tamada, O.; Shen, B.; Morimoto, N. *Mineral. J.* **1983**, *11*, 382–391.
(38) Shen, B.; Kitamura, M.; Morimoto, N. Crystallogr. Soc. Jpn. **1980**, Abs. 1–20.
(39) Li, H.; Liu, W.; Kong, Y.; Fu, P. *Kexue Tangbao* **1981**, *10*, 590–592.
(40) Shen, B.; Tamada, O.; Kitamura, M.; Morimoto, N. *Am. Mineral.* **1986**, *71*, 1455–1460.
(41) Janney, D. E.; Banfield, J. F. *Am. Mineral.* **1998**, *83*, 799–810.

(redistribution of Fe and Li onto M(1) and M(2) sites, twinning, possible intergrowth of 2 and 3 M supercells), we have not been able to precisely determine, from powder X-ray diffraction alone, the atomic positions within our oxidized samples. This will be the objective of future neutron diffraction work.

Acknowledgment. UMICORE (Belgium) is gratefully acknowledged for funding the work of S. Hamelet through a CNRS contract. Nadir Recham is warmly acknowledged for his help with the preparation of the Fe_2SiO_4 fayalite powder. Prof. Clare Grey, Univ. Cambridge, U.K., is acknowledged for fruitful discussions.